Comptes Rendus

Chimie

Ahmed Amine Azzaz, Mejdi Jeguirim, Evan A. N. Marks, Carlos Rad,
Salah Jellali, Mary-Lorène Goddard and Camelia Matei Ghimbeu

Physico-chemical properties of hydrochars produced from raw olive pomace using olive mill wastewater as moisture source

Sustainable Biomass Resources for Environmental, Agronomic, Biomaterials and Energy Applications 1 / *Ressources de biomasse durables pour des applications environnementales, agronomiques, de biomatériaux et énergétiques 1*

Physico-chemical properties of hydrochars produced from raw olive pomace using olive mill wastewater as moisture source

Ahmed Amine Azzaz[*, a, b], **Mejdi Jeguirim**[a, b], **Evan A. N. Marks**[c], **Carlos Rad**[d], **Salah Jellali**[e], **Mary-Lorène Goddard**[f, g] **and Camelia Matei Ghimbeu**[a, b]

[a] Université de Haute-Alsace, CNRS, Institut de Science des Matériaux de Mulhouse (IS2M) UMR 7361, F-68100 Mulhouse, France

[b] Université de Strasbourg, F-67081 Strasbourg, France

[c] CT BETA, Universitat de Vic – Universitat Central de Catalunya, Carrer de la Laura 13, 08500 Vic, Spain

[d] Composting Research Group UBUCOMP, Universidad de Burgos, Faculty of Sciences, Pl. Misael Bañuelos s/n, 09001 Burgos, Spain

[e] PEIE Research Chair for the Development of Industrial Estates and Free Zones, Center for Environmental Studies and Research (CESAR), Sultan Qaboos University, Al-Khoud 123, Oman

[f] Université de Haute-Alsace, Université de Strasbourg, CNRS, LIMA UMR 7042, Mulhouse, France

[g] Université de Haute-Alsace, LVBE, EA-3991 Colmar, France

E-mails: amine.azzaz@uha.fr (A. A. Azzaz), mejdi.jeguirim@uha.fr (M. Jeguirim), evan.marks@uvic.cat (E. A. N. Marks), crad@ubu.es (C. Rad), s.jellali@squ.edu.om (S. Jellali), mary-lorene.goddard@uha.fr (M.-L. Goddard), camelia.ghimbeu@uha.fr (C. Matei Ghimbeu)

Abstract. In this study, we assessed the transformation of raw olive pomace into carbon-rich material using olive mill wastewater (OMWW) as the liquid medium for the hydrothermal carbonization (HTC) process. The findings were compared accordingly with the use of distilled water (DW), which is the conventional practice. The use of OMWW as a liquid matrix enhanced the hydrochar yield, but volatile matter, fixed carbon content, and O/C and H/C ratios followed a decreasing trend. Furthermore, for an HTC temperature of 220 °C, the use of OMWW considerably increased the high heating value of the hydrochars from approximately 24.2 MJ/kg to 31.6 MJ/kg. According to the van Krevelen diagram of feedstock and derived hydrochars, dehydration was the predominant carbonization reaction for both liquid sources. Morphological characterization of both sets of hydrochars indicated the generation of specific carbon nuclei when using DW while OMWW led to the creation of hydrochar with a less

---

* Corresponding author.

homogeneous surface. Structural analysis revealed the heterogeneous aspect of the hydrochar surface with an abundance of crystallized metal-based inorganic salts.

1. Introduction

Over the past few decades, lignocellulosic biomasses have been valorized as precursor materials for energy (heat production), environmental technology (pollutant removal), and agronomic (nutrient recovery) applications [1,2]. The selection of a suitable conversion method for these biomasses depends strongly on the properties of the raw feedstock, the available pretreatment techniques, and logistics and targeted objectives. For instance, biological conversion is very sensitive to feedstock composition since the activity of microorganisms can be inhibited by toxic substances [3]. In addition, these processes require long residence times, resulting in higher volumes and operating costs [4]. On the contrary, the residence time of thermochemical processes varies from minutes to hours and does not rely on microorganisms [5]. This constitutes a significant advantage for the treatment of heterogeneous raw materials (e.g., organic wastes, sewage sludge, etc.).

Among thermochemical processes, slow pyrolysis has the advantage of producing three fractions: liquid (bio-oil) and gaseous (syngas) residues, which can be upgraded to biofuels, and a solid residue (biochar), which can be used in various applications such as soil amendment [6]. However, this solid fraction does not exceed 35%, limiting the economic viability of biochar production [7]. In addition, this process can be energy-intensive when the feedstock biomass has a high moisture content (greater than 70%). This property is common to industrial organic wastes of interest such as agrifood, paper, and woodcrafts. Therefore, a drying step is required [8].

As a consequence, hydrothermal carbonization (HTC) is a promising alternative to the pyrolysis process as it (i) avoids the costly drying step, (ii) reduces energy consumption due to the lower temperature range (180–350 °C) used, and (iii) generates in pressurized water higher yields of carbon-rich solid residue, namely, hydrochars (up to 60% on dry basis (db, %)). These carbonaceous materials are biologically and chemically more stable with a high carbon sequestration potential over decades compared to carbon products generated by slow pyrolysis [9]. Additionally, HTC usually leads to the formation of carbonaceous materials with significant mineral content, interesting concentrations of surface functional groups, and attractive morphological aspects [10]. In fact, hydrochars produced from lignocellulosic materials are characterized by a significant concentration of surface functional groups, which could be exploited either for pollutant uptake by different media or as initial feedstock for the production of high-rank carbonaceous materials. Therefore, and owing to such interesting properties, the use of hydrochars in multiple applications has been considered in other studies. These applications include supercapacitors; synthesis of Li-, S-, and/or Na-ion batteries [11]; CO_2 and H_2 gas storage [12]; soil amendment [13]; and wastewater treatment [9].

Olive oil by-products (raw olive pomace (ROP) and olive mill wastewater (OMWW)) are generated in significant amounts after the milling process. In particular, the Mediterranean region contributes to the annual generation of about 12.2 Mt solid ROP and 30 Mm^3 OMWW [14]. In various countries, these wastes are usually discharged into natural water bodies, causing severe damage and threat to the ecosystem as well as being a source of social malaise [15,16]. The sustainable management of these wastes has emerged as an urgent challenge for the purpose of not only protecting the environment but also exploiting the energetic, environmental, and agronomic potential of these organic wastes [17–21].

The HTC of ROP wastes has been tested at the laboratory scale under various experimental conditions [22–25]. The main aims of these investigations were to (i) understand the synthesis of valuable syngas, (ii) test the pretreatment of biomasses leading to carbon materials with high energetic properties, and (iii) explore the generation of interesting surface characteristics for application as adsorbents in liquid or gaseous media. All these studies have used distilled water (DW) as the moisture source during the HTC process. In the current paper, in a novel applica-

tion, OMWW is used as the liquid source for the ROP wastes. This new approach takes advantage of the huge amount of organic matter as well as minerals present in OMWW for a possible enhancement of the physico-chemical properties of the derived hydrochars. Therefore, the main objective of this work is to investigate OMWW as a liquid medium for the carbonization of ROP and to analyze its effect on hydrochar properties. This study includes an in-depth physico-chemical characterization comprising various complementary analyses. Such an understanding of the material properties is crucial to their ultimate application in agriculture in the form of fertilizers as well as efficient adsorbents of organic and mineral pollutants.

2. Materials and methods

2.1. *Raw feedstock: ROP and OMWW*

In this study, the ROP and OMWW were collected from a three-phase olive mill located in the city of Touta in North East Tunisia. The ROP was placed in airtight bags and aired periodically at ambient temperature. The liquid waste was kept in glass bottles during the experimental campaigns and was stored at 4 °C.

2.2. *HTC experiments*

The HTC experiments were performed in the presence of DW and OMWW as liquid sources. In these experiments, a solid–liquid mixture was prepared at a 1:9 ratio, corresponding to 1 g of ROP and 9 mL of the moisture source (DW or OMWW) and was placed in a 100 mL bomb calorimeter (Top Industrie, Vaux-le-Pénil, France). In accordance with typical experimental conditions, the calorimeter vessel was sealed hermetically, heated at a 10 °C/min rate using a programmable stove (Memmert, Schwabach, Germany), and kept for an isotherm period of 24 h at the three designated experimental temperatures of 180, 200, and 220 °C. The experimental conditions were chosen according to an optimization study presented in our previous papers, where HTC was performed in autogenous inner pressure atmosphere [9,10]. The hydrochars produced were accordingly named as follows: T-ROP and T-ROP + OMWW when using DW and OMWW as the moisture source, respectively,

where T is the process temperature (°C). After carbonization, the by-product was filtered using a vacuum pump through 0.45 μm Whatman® filter paper (VWR, Leuven, Belgium). The recovered solid fraction was dried overnight at 105 °C and then weighed and stored in a glass flask for later characterization. The liquid fractions were also recovered. They were filtered twice using 0.2 μm polypropylene syringe filters (VWR, Leuven, Belgium) and then stored in 10 mL glass vials at 4 °C. All experiments were performed in triplicate. Statistical analyses were conducted using R v3.6.1 [26]. An analysis of variance (ANOVA) of each testable parameter was carried out to establish differences between treatments, and then Tukey multiple comparisons (post hoc) were made using multcomp::glht.

2.3. *Hydrochar characterization*

2.3.1. *Solid yield determination*

To determine the solid yield (Y_{HC}, %), two methods were applied according to the liquid source used. In the case where DW was used as the carbonization medium, the final solid yield was calculated as follows:

$$Y_{HC}(\%) = m_{HC}/m_{FS} \times 100. \qquad (1)$$

On the other hand, the use of OMWW implies the addition of further organic matter to the carbonization medium, which should be taken into account according to (2):

$$Y_{HC}(\%) = m_{HC}/(m_{FS} + m_{S,OMWW}) \times 100, \qquad (2)$$

where m_{HC} (g) is the dry solid mass recovered after carbonization, m_{FS} is the initial feedstock mass (g), and $m_{S,OMWW}$ is the solid fraction present in the OMWW estimated as 7.9% (db, %) according to the TAPPI/ANSI T 412 om-16 method [27]. The resulting solid fraction is the subject of later solid-phase chemical characterizations.

2.3.2. *Proximate and ultimate analysis*

Proximate analysis was performed to determine fixed carbon, volatile matter, and ash contents of the hydrochars. The thermogravimetric analysis (TGA) procedure that was applied was described in our previous studies [10]. A Flash 2000 CHNS-O Elemental Analyzer (Thermo Fisher Scientific, Cambridge,

UK) was used to determine the elemental composition. Furthermore, the mineral composition of ROP, OMWW, and the derived hydrochars was determined using multiple extraction methods. The total nitrogen contents were determined according to the modified Kjeldahl method (ISO 1995). Soluble contents of K^+, Na^+, Mg^{2+}, Ca^{2+}, $N-NH_4^+$, and soluble phosphorus were assessed according to the analytical method described by Thomson and Leege [28].

2.3.3. *Morphological and structural properties*

A high-resolution scanning electron microscopy (SEM) analysis was performed using a Philips XL30 microscope coupled with an energy-dispersive X-ray spectroscope (EDS; Oxford Instruments, Oxfordshire, UK) to determine the atomic composition of the hydrochars. Powder X-Ray diffraction (XRD) was employed to identify the crystalline phases in the prepared hydrochars. It was carried out by a PANalytical X'Pert powder diffractometer (Malvern, UK) equipped with a copper anode. Phase identification was conducted using the database from the International Center for Diffraction data (Crystallography Open Database; Graulis *et al.* [29]) on the PANalytical HighScore software.

2.3.4. *Bulk and surface chemistry*

The bulk quantitative characterization of the hydrochars produced was performed by two methods. First, pH at zero-point charge (pH_{ZPC}) was determined to gain an overall idea of the dominating surface charge. Then, acidic groups were quantified using the Boehm titration method. Both methodologies are described thoroughly in the literature [30]. Second, the surface chemistry was analyzed using a spectroscopic method (Fourier transform infrared (FTIR)). The FTIR spectra were acquired by an Equinox 55 Bruker spectrometer (Ettlinger, Germany). For each sample, an exact biochar-to-KBr mass ratio of 1/200 was ground in a mortar and pressed into a 1 cm diameter disk at a pressure of 3.5 tons. The disk-like sample was then analyzed at a spectral resolution of 4 cm^{-1}, which was measured between 4000 and 400 cm^{-1}.

2.3.5. *Energy contents*

The energy contents of the raw feedstock and the derived hydrochars were assessed by determining the higher heating value (HHV) and the lower heating value (HHV). The HHV (MJ/kg) is defined as the amount of energy released by the complete combustion of a fuel unit, where the water vapor is assumed to be condensed and the heat recovered. The HHV (MJ/kg) is related to the energy released during the combustion of a solid without taking into account the energy of water condensation [10]. Analyses were performed using an IKA C 200 bomb calorimeter (Staufen, Germany) according to DIN 51900 in the isoperibolic reaction mode. The LHV was calculated on the basis of the values of the HHV and the percentages of moisture and hydrogen (at dry base).

2.4. *Liquid characterization*

The quality of the final liquid medium after HTC was assessed by determining the chemical oxygen demand (COD, g O_2/L). The dichromate titrimetric method was used according to the protocol given by Moore *et al.* [31].

The organic composition of the process water after HTC was determined by gas chromatography coupled with mass spectrometry (GC–MS). The equipment used consists of a GC-2010 gas chromatograph coupled with a GC-QP2010 mass spectrometer (Shimadzu, Tokyo, Japan). After filtration on 0.2 µm regenerated cellulose syringe filters, samples were diluted 10 times in ultra-pure water (resistivity 18.0 µΩ·cm). As internal standard, 50 µL of 10 µg/mL phenoxyacetic acid aqueous solution was added to 30 µL of the diluted solution; then, the samples were freeze-dried. Afterward, they were chemically derivatized and immediately analyzed by GC–MS as stated by Jeguirim *et al.* [17]. The peak assignment was carried out using an internal compounds' library as well as by the mass spectral library NIST 17.

3. Results and discussion

3.1. *Carbonization yield*

The effect of temperature and variation in the carbonization medium on the final hydrochar yield is presented in Figure 1. The carbonization of ROP in water and in OMWW at increasing temperatures led to a progressive decrease in the final yields of hydrochars. In fact, the hydrochar percentage decreased from 54.90% to 37.50% and from 41.87%
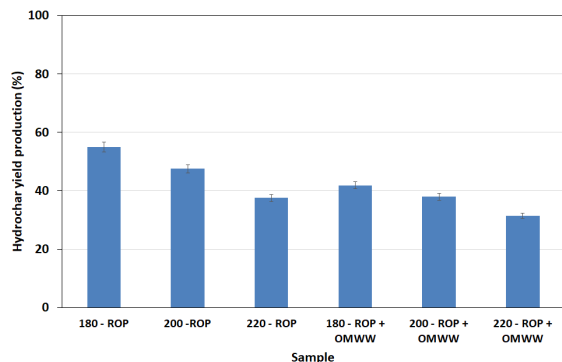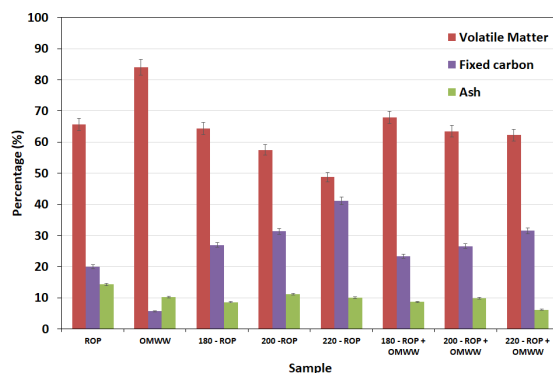
Figure 1. Final solid yields of the hydrochars derived from ROP in the presence of distilled water and OMWW as carbonization media at different temperatures (reported error is standard deviation).

Figure 2. Proximate analysis for ROP, OMWW's solid fraction, and derived hydrochars in the presence of distilled water and OMWW as carbonization media at different temperatures (reported error is standard deviation).

to 31.37% when the carbonization temperature increased from 180 to 220 °C for ROP + DW and ROP + OMWW, respectively. This loss of solid mass with increasing temperature is attributed to the degradation of the lignocellulosic matrix of both materials as the temperature increases. Moreover, higher temperatures induce major modifications in the moisture state inside the reactor, favoring the conversion of the biomass [32]. It is also seen that the type of liquid matrix significantly affects the hydrochar production yields. Here, at carbonization temperatures between 180 and 220 °C, the degradation rate of ROP in the solid fraction decreased from 17.5% to 10.5% when using DW and OMWW as moisture sources, respectively. Similar findings were reported by Li *et al.* [33] when studying the impact of liquid wastes on the HTC of different municipal wastes. In fact, reported results suggest that the carbonization of yard waste in the presence of landfill leachate containing significant contents of organic matter as the moisture source enhanced the dewaterability of solids as a function of time and decreased the recovery of the final solid fraction.

3.2. *Proximate, ultimate, and elemental analyses*

3.2.1. *Proximate and ultimate analyses*

Proximate analysis was performed for ROP and the produced hydrochars in the presence of DW and OMWW, respectively. The results depicted in Figure 2

show that ROP is characterized by a high content of volatile matter (66%) with relatively low percentages of fixed carbon and ash of 20% and 14%, respectively. On the other hand, OMWW contains volatile matter, fixed carbon, and ash of approximately 84%, 6% and 10%, respectively [10]. When using DW, the produced hydrochars exhibit a decrease in volatile matter content from 64% to 49% for 180-ROP and 220-ROP, respectively. On the other hand, a significant increase in the fixed carbon content is observed, ranging from 28% to 41% for the same samples. This observation is attributed to the effect of temperature increase on the recombination and the polymerization of the light volatile matter into more condensed carbon content. Similar findings were reported by Missaoui *et al.* [22] when investigating the HTC of olive pomace at different temperatures. In this case, the volatile matter content decreased from 71.6% to 61.0% and the fixed carbon increased from 23.6% to 36.2% at treatment temperatures between 180 and 250 °C, respectively.

Conversely, the addition of OMWW as the moisture source for the carbonization of ROP did not enhance the quality of the final hydrochars. In fact, despite the increase in fixed carbon content of approximately 8%, the volatile matter contents remained relatively high and varied between 68% and 62% at carbonization temperatures between 180 and 220 °C, respectively (Figure 2). These results confirm that the slight decrease in the hydrochar yields when OMWW

is added instead of DW is due to the difference in the volatile matter content (see Figure 1). The results suggest that the high content of volatile matter in both ROP and OMWW led to a decrease in their conversion rate into more stable carbon content. It is worth mentioning that in both cases, when using either DW or OMWW, the ash contents decreased with increasing temperature compared to that of the solid feedstock (Figure 2). Indeed, compared to ROP, these contents decreased by approximately 4% and 8% for an HTC temperature of 220 °C in the presence of DW and OMWW, respectively. Similar studies investigating the HTC of olive pomace suggested that an increase in treatment temperature enhances the ash content as minerals are more likely to be incorporated into the rearranged and more stable aromatic structure [22]. In our current study, it is possible that the degradation of the ROP as well as the physico-chemical properties of OMWW resulted in the production of highly scouring molecules, which contributed to the degradation of the lignocellulosic matrix and the release of minerals and organic contents from the solid fraction.

To have a clearer idea about the significance of the previous results, statistical tests were performed on the reported parameters (Figure S1-b). Regarding ash contents, there were generally no large or statistically significant differences between the measured samples. However, volatile matter—which was highest in the OMWW—showed a decreasing trend in values with increase in HTC temperature for both T-ROP and T-ROP + OMWW samples (Table 1). As expected, fixed carbon exhibited the exact opposite trends to those of volatile matter. It was lowest in OMWW and increased with treatment temperature (Figure S1-b).

Ultimate analysis was performed for ROP feedstock as well as the resulting hydrochars and the solid fraction of OMWW. The results are shown in Table 2. Initially, the ROP had percentages of carbon and oxygen of about 43% and 47%, respectively, which are similar to the majority of lignocellulosic-based feedstocks reported in the literature [34]. As for the solid fraction of OMWW, carbon and oxygen contents were 57% and 32%, respectively. When the carbonization temperature was increased for both moisture sources, an increase in C and a decrease in O percentages were observed. In fact, when using DW, C% increased from 43% to 64% and O% decreased from 47% to 27% for ROP and 220-ROP samples, re-

spectively. On the other hand, this modification was further intensified when adding OMWW to the carbonization media as carbon and oxygen percentages for 220-ROP + OMWW were 68% and 20%, respectively. Nevertheless, the observed modifications in the H and N contents of the raw and carbonized materials were found to be low, with a maximum variation of ±2.37% and ±1.02%, respectively. Such behavior could be ascribed to two synergistic effects. (i) Owing to its high carbon (Table 2) content, OMWW could have contributed to the impregnation of a small fraction of volatile organic compounds into the ROP. An increase in the carbonization temperature resulted in the condensation of the added carbon, which enhanced the final carbon content compared to the use of DW. (ii) The high acidity of the OMWW accelerated the defragmentation of cellulose and hemicellulose, which resulted in a noticeable reduction in the oxygen percentage.

3.2.2. *NPK analysis*

One of the most important methods for the characterization of hydrochars is the determination of their content in macroelements for eventual application in agriculture. As shown in Table 3, ROP is characterized by a total nitrogen, soluble phosphorus, and potassium (NPK) content of approximately 13.2 g/kg. When the HTC is performed at increasing treatment temperatures in the presence of DW, different tendencies in mineral concentrations were found. For instance, the potassium and sodium contents decreased from 6100 to 950 mg/kg and from 580 to 136 mg/kg for ROP and 220-ROP, respectively. Similarly, hydrochar contents of phosphorus and magnesium reduced considerably from 118 to 9 mg/kg and from 175 to 119 mg/kg for the same samples, respectively. However, an opposite trend was detected for the calcium content as it apparently increased from 560 to 860 mg/kg for ROP and 220-ROP, respectively. On the other hand, the hydrochars produced with OMWW as the carbonization medium showed the same global tendency in terms of mineral composition. Here, the global NPK soluble content decreased from 13.16 to 6.77 g/kg for ROP and 220-ROP + OMWW, respectively.

In contrast, a significant increase in the potassium contents was observed from 6100 mg/kg for ROP to 8000 and 9000 mg/kg when carbonization was carried out in the presence of OMWW at 180 and 200 °C,

Table 1. ANOVA table for study parameters with degrees of freedom (DF), sum of squares, residuals, *F*-test value, and significance

Parameter	DF	Sum sq.	Resid. DF	Resid. sum sq.	F	Sig.
Solid yield	5	1040	12	17	143.4	***
Ash	7	113	16	71	3.6	*
Volatile matter	7	2086	16	42	111.2	***
Fixed carbon	7	2235	16	130	39.2	***
Phenolic	7	217088	16	76361	6.5	***
Carboxylic	7	232293	16	39230	13.5	***
Lactonic	7	681354	16	6403	243.2	***
pH_{ZPC}	7	13.7	16	0.8	40.7	***

Significance codes are as follows: $p < 0.0001$, "***"; $p < 0.05$, "*".

Table 2. Ultimate analysis (wt.%) of the ROP, OMWW's solid fraction, and derived hydrochars in the presence of distilled water and OMWW as carbonization media at different temperatures

Samples	C (%)	O (%)	H (%)	N (%)	S (%)
ROP	42.80	46.51	5.65	2.01	0.23
OMWW*	56.75	31.74	7.90	2.72	0.22
180-ROP	56.13	34.91	5.91	0.99	0.12
200-ROP	62.58	28.00	5.89	1.37	0.13
220-ROP	64.37	26.76	5.47	1.27	0.14
180-ROP + OMWW	62.73	25.19	8.02	1.88	0.18
200-ROP + OMWW	64.98	23.86	7.26	1.63	0.16
220-ROP + OMWW	67.90	20.24	7.64	1.86	0.07

*Analysis performed on the solid fraction of OMWW.

respectively (Table 3). The highest mineral content was found for the sample 200-ROP + OMWW with an estimated total of 11.851 g/kg. Although all the recovered hydrochars had a lower mineral content compared to the solid fraction of OMWW (total mineral content of 70.5 g/kg), they are still characterized by larger carbon contents and lower volatile matter. These properties could be beneficial in both energetic and agricultural applications [10].

When studying the fate of minerals in the solid fraction after HTC, controversial explanations and findings are encountered in the literature. The HTC of biomass is characterized by a very complex process that involves both synergistic and antagonistic reactions, which depends mainly on the process temperature as well as the pH of the medium. Although the first parameter is permanently controllable, the solution acidity is contingent on the highly variable physico-chemical properties of the feedstock. Therefore, the impact of tuning these two parameters on the final mineral composition is relatively unpredictable. For instance, Chen *et al.* [35] reported an increase in nitrogen and phosphorus and a decrease in potassium solid concentrations with increase in carbonization temperature when the liquid pH varies between 3.52 and 4.83. The increase in solids in acidic media was ascribed to a possible deposition of soluble minerals on the hydrochar during the recombination reaction. Similarly, Smith *et al.* [36] reported an increase in the mineral composition of hydrochars produced from willow wood at two different temperatures. When the HTC is increased from 200 to 250 °C, they demonstrated an enhancement in magnesium, phosphorus, and calcium concentrations of approximately 11%, 31%, and 15%, respectively, while the potassium content decreased by about 46%. Conversely, Huang *et al.* [37] reported that the increase in the HTC temperature significantly reduced the presence of minerals in the final hydrochars produced from the cocarbonization of pine sawdust and plastic polymer granules. In fact, significant leaching of calcium, magnesium, potassium, and sodium in the liquid fraction was noted at the rates of 98.59%, 97.66%, 92.32%, and 87.43%, respectively, following the conversion of raw sawdust to hydrochar at 260 °C. The authors suggested that an increase in the carboniza-

Table 3. Elemental composition (wt.%) of ROP and hydrochars produced from HTC in the presence of distilled water and OMWW at different temperatures

Samples	K (mg/kg)	Na (mg/kg)	Ca (mg/kg)	Mg (mg/kg)	P (mg/kg)	N_{Total} (mg/kg)	Sum of minerals (mg/kg)
ROP	6100.00	580.00	560.00	175.00	118.00	6950.00	14483.00
OMWW*	44000.00	3700.00	1421.00	1744.00	2034.00	17600.00	70499.00
180-ROP	1350.00	148.00	606.00	116.00	81.30	7330.00	19901.30
200-ROP	1650.00	156.00	438.00	103.00	52.20	7930.00	10329.20
220-ROP	950.00	136.00	860.00	119.00	9.21	9260.00	11334.21
180-ROP + OMWW	8000.00	620.00	283.00	347.00	110.00	1370.00	10730.00
200-ROP + OMWW	9000.00	840.00	293.00	448.00	50.80	1220.00	11851.80
220-ROP + OMWW	1450.00	148.00	22.10	11.40	31.40	5290.00	6952.90

*Solid fraction of OMWW.

tion temperature led to an acceleration in the auto-ionization of the water molecule toward an abundance of hydronium (H_3O^+) concentration in the media. It was presumed that H_3O^+ ions catalyzed the solubilization of the salts embedded in the lignocellulosic materials and their recovery in the liquid fraction.

Another observation that must be highlighted is the abrupt decrease in the contents of some minerals when the carbonization temperature increases from 200 to 220 °C for both media. As an example, in the case where OMWW is the moisture source, potassium, sodium, and calcium decreased by about 84%, 82%, and 92%, respectively. These minerals are generally incorporated into the biomass as part of their lignocellulosic matrix. According to the TGA results (Supplementary material, Figure S2), the degradation of cellulose and hemicellulose most likely started in the temperature range between 200 and 230 °C. The degradation of polymers led to the widening of matrix pores and then the liberation of the minerals from solid to liquid and gaseous phases.

3.3. *Energy contents*

Calorific measurements are considered as an important method for investigating the quality of the hydrochars produced. According to the results presented in Table 4, the ROP's HHV and LHV are 14.73 and 13.39 MJ/kg, respectively, which are similar to those of common biomasses such as eucalyptus wood (16.26 MJ/kg; Elaieb *et al.* [38]) and

chestnut shell (15.49 MJ/kg; Özçimen and Ersoy-Meriçboyu [39]). The HHV of the OMWW solid fraction is 26.55 MJ/kg. Increases in the process temperature of the ROP HTC in the presence of either DW or OMWW significantly increased its HHV and LHV. Indeed, the highest HHV and LHV values are shown for an HTC temperature of 220 °C (LHV 29.88 and HHV 31.62 MJ/kg, respectively, are used as the moisture media. Thus, the use of OMWW instead of DW permits the production of hydrochar with an improved HHV (about 6% higher). The increase in calorific capacity is generally attributed to the significant increase in the O/C ratio for both liquid media [9]. Nevertheless, it has been reported that the increase in moisture acidity enhanced the final HHV of hydrochars. In fact, cellulose and hemicellulose are generally characterized by low calorific capacities (17.28 MJ/kg and 16.81 MJ/kg, respectively; Zhao *et al.* [40]). These were transformed into more stable components with lower oxygen contents when hydrothermally carbonized at low pH values [41]. The condensation and the repolymerization of the generated by-products lead to the formation of bitumen-like and humic-acid-like materials, which end up readhering to the highly calorific lignin matrix (25.51 MJ/kg; [40]). This hardly occurs at a carbonization temperature of 220 °C.

According to the literature, various possible mechanisms could be involved during the HTC of biomasses into hydrochars such as deamination, dehydrogenation, demethylation, deoxygenation, dehydration and/or decarboxylation [42,43]. To pre-

Table 4. Calorific quantities for ROP and derived hydrochars in the presence of distilled water and OMWW as carbonization media produced at different temperatures

Samples	ROP	OMWW*	180-ROP	200-ROP	220-ROP	180-ROP + OMWW	200-ROP + OMWW	220-ROP + OMWW
HHV (MJ/kg)	14.73	26.55	22.80	24.06	24.21	27.74	29.58	31.62
LHV (MJ/kg)	13.39	24.76	21.43	22.70	22.94	25.91	27.92	29.88

*Solid fraction of OMWW.

dict the possible mechanism, a van Krevelen diagram depicting the O/C versus H/C atomic ratios is presented in Figure 3. The atomic ratios corresponding to ROP suggest that long-chain polysaccharides such as cellulose and hemicellulose are its major components [44,45], which is further confirmed by its similarity to a pure cellulose composition (Figure 3). The increase in the carbonization temperature of ROP from 180 to 220 °C in the presence of water caused a decrease in both O/C and H/C ratios from 0.45 to 0.30 and from 1.26 to 1.02, respectively (Figure 3). A similar tendency was observed when OMWW was used as the moisture source since O/C and H/C ratios decreased from 0.28 to 0.22 and from 1.52 to 1.35 for the same carbonization temperatures, respectively. Moreover, it could be remarked that in the presence of OMWW, hydrochars exhibited higher H/C and lower O/C ratios compared to those produced using DW. It is possible that the addition of OMWW enhanced the organic charge as well as the acidity of the media by increasing the proton concentrations in the solution and subsequently on the surface of the carbonaceous materials, which explains the difference in H/C ratios. According to the evolution of H/C and O/C atomic ratios, it could be suggested that dehydration is the dominating mechanism for the HTC of ROP in the presence of DW or OMWW. This indicates the cleavage of surface functional groups of ROP in acid-catalyzed media, yielding water as the main carbonization by-product [46].

3.4. *Morphological and structural properties of hydrochars*

3.4.1. *Morphological properties*

The morphological structure of ROP after HTC with different liquid media was assessed using SEM imaging coupled with EDS analysis. Initially, ROP

presented a rough and kinky surface with no significant porosity (Figure 4). After HTC, the resulting solids showed significantly different structural characteristics. In fact, in the presence of DW, the ROP-derived hydrochars were sphere-like carbon structures of different diameters. According to SEM images, the sphere diameter varies between 0.49 and 1.69 μm for 180-ROP; 57% of these particles have a diameter between 0.67 and 0.84 μm (Figure 4). It has been reported that these structures possess an internal solid and porous morphology [50], where their size depends mainly on the carbonization temperature and time [51]. The formation mechanism of these spheres could be attributed to the degradation of hexose and pentose present in the lignocellulosic material at increasing temperatures through a dehydration reaction. The degradation of these two monosaccharides leads to the formation of 5-hydroxymethylfurfural (5-HMF) and furfural, respectively. Studies suggest that for an extended reaction time where high temperatures are maintained, these organic compounds are polymerized and highly aromatized, which eventually allows the carbon to condense in the form of microspheres [49,52]. When the carbonization temperature is increased, the spherical structures become less obvious on the surface of the hydrochar at 200 °C with a relatively lower diameter varying between 0.14 μm and 1.11 μm until disappearing at 220 °C. It is worth noting that the hydrochar produced at 220 °C presented a similar apparent characteristic compared to the ROP with a very heterogeneous surface and without a porous structure.

On the other hand, the carbonization of ROP at increasing temperatures in the presence of OMWW resulted in a very different hydrochar morphology. At 180 °C, the hydrochar produced was characterized by deformed sphere-like particles. It appears that the addition of OMWW, which is more acidic than DW (pH = 4.86), affected the proper formation of the car-
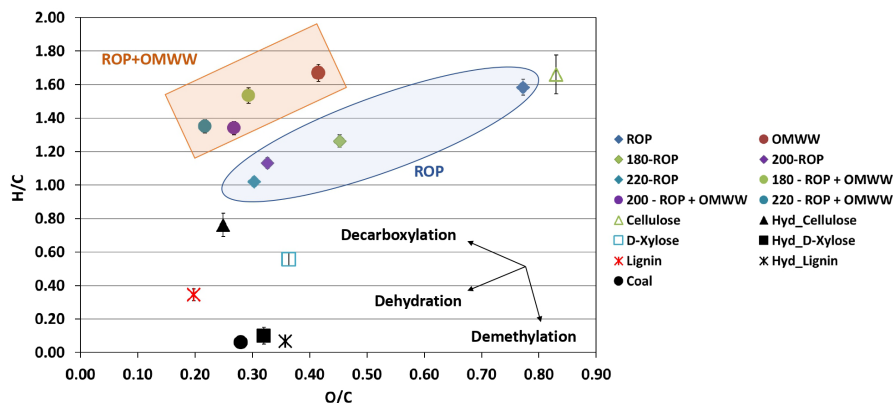
Figure 3. Van Krevelen diagram for ROP and derived hydrochar produced at various temperatures in the presence of distilled water and OMWW versus carbonaceous materials present in the literature [47–49] (reported error is standard deviation).

bon spheres as compared to the use of DW. Similar results were described by Liang *et al.* [53] when performing the HTC of starch at different pH values of process water. They found that the carbonization of starch at a pH of 1 reduced significantly the growth of the carbon nanospheres compared to a solution pH varying between 3 and 7.

According to the LaMer model related to the nucleation-growth mechanism, the development of these particles is achieved when soluble polymers derived from the degradation of the cellulose and hemicellulose reach a certain saturation point and start segregating from the liquid medium [54]. The diffusion of these species through the solid is mainly ensured by the oxygen functional groups present on the surface, leading to the growth of carbon nuclei with a hydrophilic shell and a hydrophobic core [9]. However, the presence of strong acids at significant concentrations in the process water could change the dominating surface charge and composition and inhibit the diffusion of some oxygen functional groups through the solid either by complexation or electronic repulsion, thereby stopping the growth of carbon nuclei (180-ROP + OMWW; Figure 4) [52]. This could also explain the aspect of ROP and ROP + OMWW produced at 200 and 220 °C, as an increase in carbonization temperature has been known to increase the production of organic acids that hinders the diffusion of soluble free entities such as hydroxyl and carbonyl groups inside the hydrochar matrix [53].

The modification of the moisture source and the process temperature has an impact on the mineral composition of the hydrochars as well. Initially, EDS cartography related to ROP show a uniform partition of carbon and oxygen (Figure S3-a). For both moisture sources, EDS cartography suggest an increase in the carbon partition with increasing carbonization temperature (Figure S3). Moreover, a large variety of minerals are detected in the form of a homogeneous partition for the case of sodium, magnesium, potassium, and phosphorus, while some other elements such as silica, sulfur, and calcium exhibit a certain agglomerative property. When the carbonization temperature is increased and when the moisture source is modified, the carbon contents increase while oxygen constantly decreases due to the condensation of organic matter driven by dehydration mechanisms (Figure S3). Furthermore, mineral content appears to be highly affected by the increase in carbonization temperature as the general tendency suggests a significant decrease until the disappearance of certain minerals at an HTC process temperature of 220 °C. Such behavior is attributed to the combined impact of increasing temperature and solution acidity, which contributes to the release of minerals from the solid fraction [55]. These observations are in agreement with the elementary and proximate analyses.

3.4.2. *Structural properties*

In the presence of DW or OMWW, the impact of the HTC process on the structural properties of
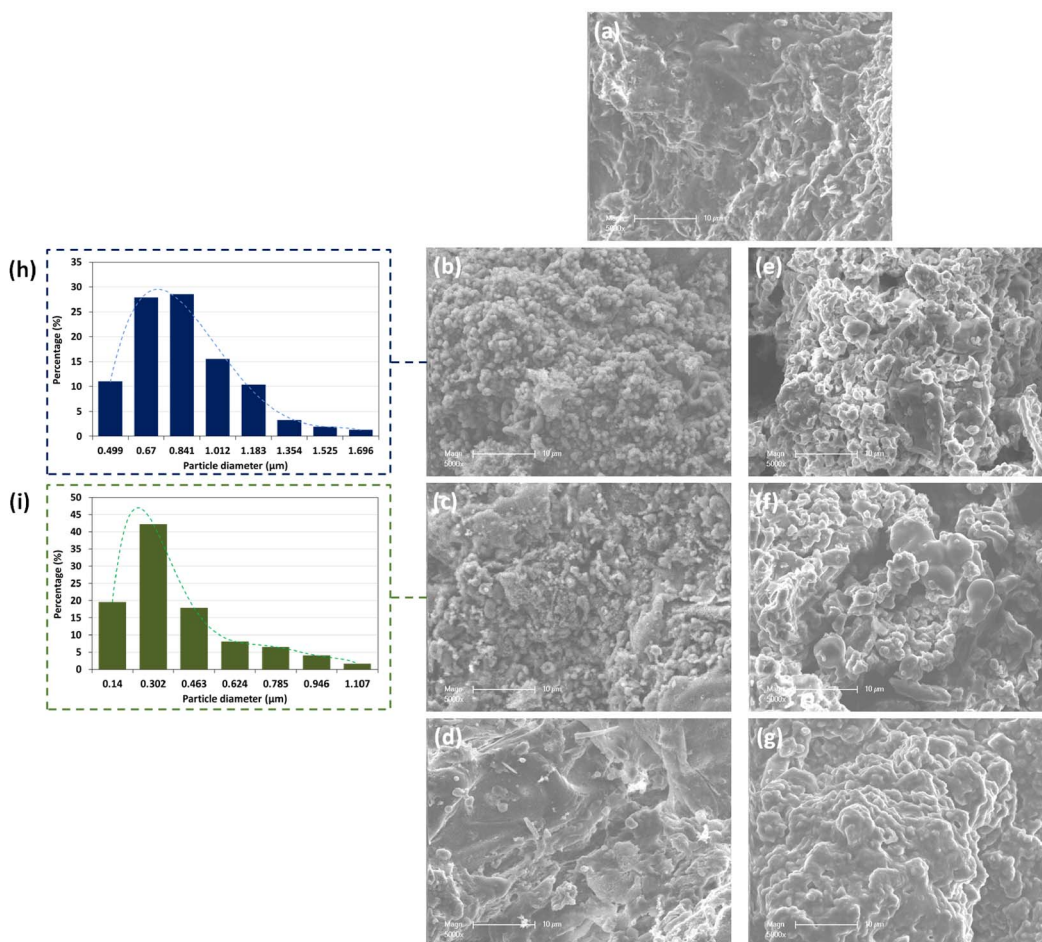
Figure 4. SEM images of (a) ROP and derived hydrochars using (b–d) distilled water and (e–g) OMWW as carbonization media produced at 180, 200, and 220 °C, respectively, and the spherical particle size distribution for (h) 180-ROP and (i) 200-ROP.

the hydrochars produced was examined using the XRD technique. First, ROP showed a diffractogram typical of a lignocellulosic material with an amorphous cellulose I broad peak at 22.6° (2θ) [30] as well as the existence of some minerals in crystalline form such as SiO_2, CaC_2O_4, $CaCO_3$, and KCl. After increasing the carbonization temperature up to 200 °C, no major modifications in the organic skeleton were noted. This suggests that the cellulosic structure was preserved (Figure 5). Moreover, peaks related to calcite ($CaCO_3$; at 32.35°, 36.40°, and 38.38° (2θ)) disappeared, while others corresponding to calcium phosphate ($Ca_3[PO_4]_2$) emerged. This could be attributed to a rearrangement reaction as

calcium oxalate is usually found in lignocellulosic materials as monohydrates and dihydrates in a rare form [56]. It is presumed that H_2O molecules coordinate the crystalline structure between oxalate and calcium ions [57]. Therefore, the attenuation of calcium oxalate peaks along with other calcium-based crystals could be related to the dehydration reaction driving the carbonization process of ROP. When the carbonization temperature is further increased to 220 °C, the peak at 22.6° (2θ) disappears, which suggests that the degradation of the cellulose in ROP takes place between 200 and 220 °C, confirming the reported TGA findings (Figure S2). Similar observations were made by Zhang *et al.* [58]
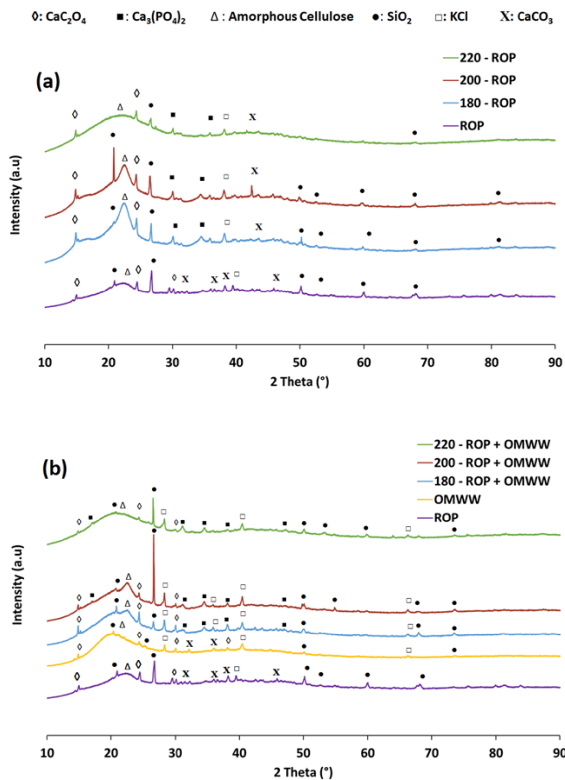
Figure 5. XRD diffractograms for the ROP and its derivative hydrochars in the presence of (a) distilled water and (b) OMWW as moisture sources at different hydrothermal carbonization temperatures.

when studying the HTC of corncob residues at different temperatures. They suggested that the cellulosic structure of the feedstock reached its integrity limit at 230 °C.

On the other hand, the use of OMWW as a carbonization medium accelerates the degradation process of the cellulose even at relatively low temperatures (Figure 5). The OMWW has a structure similar to that of the ROP with the exception of the characteristic cellulose I peak, where a slight shift is seen from 22.6° to 19.6° (2θ), respectively. Despite the fact that this peak is attributed to the same amorphous structure as that which is present for ROP, the OMWW peak slightly precedes the ROP peak, which suggests a possible alteration in the hemicellulose structure related to the milling process. When the HTC is carried out at 180 and 200 °C, a small decay is noted at
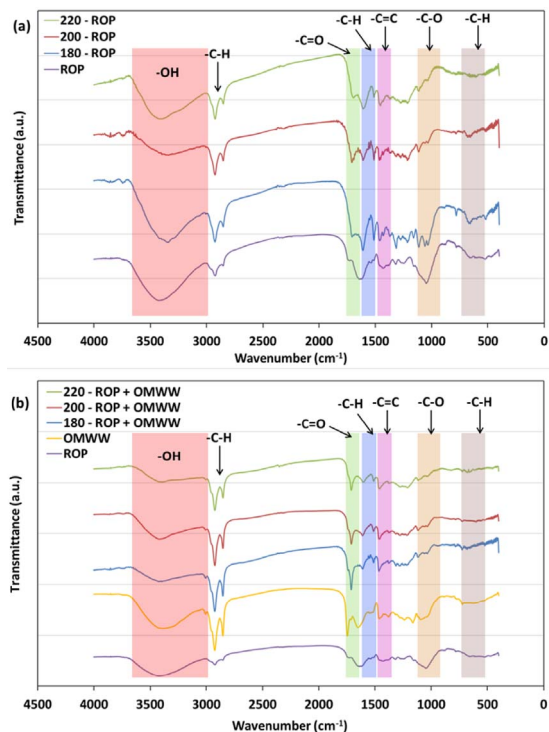

Figure 6. FTIR spectra for ROP and derived hydrochars when using (a) distilled water and (b) OMWW as carbonization media produced at different temperatures.

19.6° (2θ) related to the cellulosic fraction of OMWW. Moreover, when OMWW is used instead of DW, it can be clearly seen that the amorphous cellulose structure of ROP hydrochars becomes less relevant. Owing to its high acidity, the OMWW seems to accelerate the decomposition of cellulose into more amorphous forms.

3.5. *Surface chemistry of hydrochars*

To assess the impact of modifying the carbonization media on the surface chemistry of ROP and its derived hydrochars produced at different temperatures, a set of three characterization techniques were employed: FTIR, Boehm titration, and surface pH_{ZPC}.

The FTIR spectra of the feedstocks and their respective hydrochars produced at different temperatures are presented in Figure 6. The results suggest that the initial biomass and derived hydrochars possess a rather heterogeneous surface with multiple
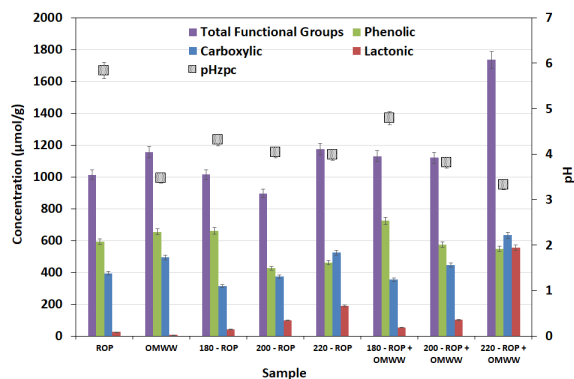
Figure 7. Acidic functional groups and surface pH$_{ZPC}$ of the ROP and the hydrochars produced from the HTC at different temperatures in the presence of distilled water and OMWW (reported error is standard deviation).

acidic and basic functional groups. For both cases, when DW or OMWW is used as the carbonization medium, common functional groups could be found: hydroxyl (–OH; 3600–3200 cm^{-1}), aliphatic (C–H; 3000–2700 cm^{-1}), carbonyl and acetyl esters (C=O and C–O stretching vibrations, respectively; 1650–1600 and 1180–980 cm^{-1}), methyl and methylene aromatic groups (–CH$_2$/–CH$_3$; 1465–1320 cm^{-1}), cellulose carbonyl (C–O–C symmetric stretching; 1160–1110 cm^{-1}), and out-of-plane aromatic groups (C–H; 896–809 cm^{-1}). After carbonization, various differences were observed.

After DW was employed, peaks corresponding to hydroxyl groups decreased in intensity with increase in carbonization temperature. It has been reported that this decrease indicates the tendency of the HTC toward dehydration [49]. An increase in the peak shift from −19 to −33 cm^{-1} was detected when the carbonization temperature was increased between 180 and 220 °C, related to a vibration of the C=O hemicellulosic aromatic structure. Similar behavior was noted for aromatic C=C functional groups, where the related peak shifted by −16 to −18 cm^{-1} for the same treatment temperatures. This could be attributed to stretching in the aromatic skeleton of the lignin matrix [59]. Some deformations could also be ascribed to –CH$_2$/CH$_3$ and carbonyl C–O aromatic groups as they shifted by +4 and +11 cm^{-1} for ROP and 220-ROP, respectively.

In the case where OMWW was used as the mois-

ture source, similar tendencies were observed as the peak intensity of the O–H hydroxyl group decreased significantly until almost disappearing for the 220-ROP + OMWW sample (Figure 6). However, careful inspection of the peaks revealed a stabilization of the location of C=O, C=C, and –CH$_2$/–CH$_3$ functional groups. This result is in agreement with the outcome of the nucleation reaction as in the presence of OMWW, the ROP depolymerized structure fails to form any carbon nuclei (Figure 6b). In fact, the formation of carbon spheres is linked to a phenomenon of dehydration of specific polymers, namely, hemicellulose and polysaccharides, as this reaction implies a reduction in O/C and H/C ratios [49]. The diffusion of carbonization by-products with increasing temperature rate induces the rearrangement of condensed carbon in the form of benzene rings, which form stable groups with oxygen in the nucleus (e.g., ether, quinone, and pyrone). Moreover, the shell is composed of reactive oxygen hydrophilic functionalities (e.g., hydroxyl, carbonyl, carboxylic, and ester; Li *et al.* [52]).

To further understand the modification kinetics of the surface functional groups, Boehm titration and pH$_{ZPC}$ techniques were carried out for the raw and carbonized solids. The results are shown in Figure 7. ROP had significant contents of acidic functional groups; a large content of phenolic and carboxylic groups and a low content of lactonic groups were present. When the HTC of ROP was conducted in the presence of DW, a slight increase in the concentration of phenols was detected from 594 to 661 μmol/g for ROP and 180-ROP, respectively. Moreover, carboxylic functional group contents decreased from 394 to 313 μmol/g for the same samples, respectively (Figure 7). When the carbonization temperature was increased, opposite trends were observed as concentrations of phenolic groups decreased by approximately 30% and carboxylic functionalities increased by 67% for the carbonization reaction between 180 and 220 °C, respectively (Figure 7). On the other hand, the content of lactonic groups increased by more than sixfold when the raw material was carbonized to 220 °C, which is attributed to the effect of degradation of cellulose on the formation of highly acidic functional groups. When OMWW was added to the carbonization media, similar outcomes were noted in terms of increase in the carboxylic group concentrations and a decrease in the pheno-

lic groups. However, the content of lactonic groups increased remarkably from 190 to 556 µmol/g.

From a statistical point of view, lactonic functional groups were practically absent in the feedstocks, but increases in HTC temperature had the strong effect of increasing these groups together with a very significant increase in 220-ROP − OMWW (Table 1; Figure S1-c). Carboxylic group density also appeared to be increased with temperature, whereas the highest densities were found not only in the 220 °C hydrochars but also in OMWW. Among phenolic groups, there appeared to be a trend toward decreased densities with increase in carbonization temperature (Table 1; Figure S1-c).

Such behavior could explain the tendency of the solid pH_{ZPC} (Figure 7) where it constantly reduced with increasing carbonization temperature. The ROP had the highest value, which was statistically different from all other materials. The OMWW and hydrochars all had lower and similar pH_{ZPC} values, whereas this decreased with temperature (Figure S1-d). In fact, it decreased from 5.84 to 3.98 for ROP and 220-ROP, respectively. When OMWW was added, solid pH_{ZPC} varied from 5.84 to 3.32 for these samples, respectively. Therefore, it could be suggested that the enhancement of surface acidity was driven by both the effect of the acidic moisture source and the generation of highly protonated entities that contributed to the modification of the surface charge by adsorption, diffusion, or ion-exchange reaction between the solid and liquid fractions. In fact, a possible elimination of hydroxyl groups could be behind the relative stability of the final liquid pH, whereas it changed from 4.53 to 4.77 for 180-ROP + OMWW and 220-ROP + OMWW, respectively.

3.6. *Liquid characterization*

The characterization of the liquid fraction at the end of the HTC could be considered as an important parameter for understanding the ROP's degradation mechanism. This information is valuable when considering the possible application of ROP in agriculture. Although the reuse of the final process water in the irrigation of plants is economically very advantageous, it could pose some undesirable physicochemical hazards, leading to the irreversible alteration of soils and crops.
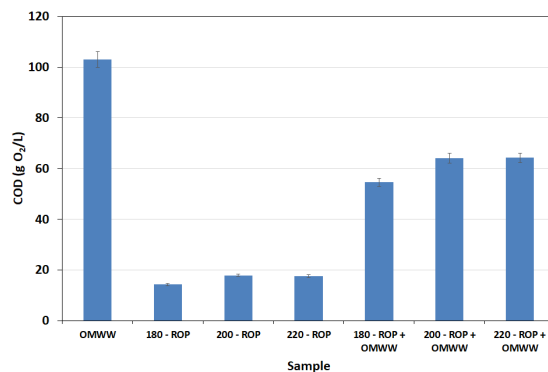
Figure 8. Chemical oxygen demand of the final liquid fraction (bio-oil) after the HTC of ROP in the presence of distilled water and OMWW at different temperatures (analysis performed in duplicate: $n = 2$; reported error is standard deviation).

The quality of the final process water has been assessed by studying the evolution of COD. The corresponding results are shown in Figure 8. When the carbonization of ROP in DW is carried out, a release of organic molecules is observed with increasing temperature since COD contents are 14.25, 17.85, and 17.55 g O_2/L for treatment temperatures of 180, 200, and 220 °C, respectively (Figure 8). This confirms our previous suggestion regarding the migration of soluble organic compounds such as fatty acids and phenols from the solid phase to the liquid fraction at increasing carbonization temperatures. These values are noticeably higher in the presence of OMWW since they reach 54.60, 64.05, and 64.20 g O_2/L for the same temperatures, respectively. Nevertheless, these COD concentrations are approximately 53% to 62% of the original OMWW content (103 g O_2/L). It is possible therefore that a significant fraction of the OMWW organic content has been incorporated into the ROP lignocellulosic matrix. This content is involved in the degradation mechanism during the HTC of the ROP. A similar outcome was noted by Li *et al.* [33] when studying municipal waste HTC in the presence landfill leachate.

To obtain proper information about the degradation mechanism of the feedstock in the presence of different moisture sources, a GC–MS analysis of final liquids was carried out following the method presented in Section 2.4. According to Table S4,
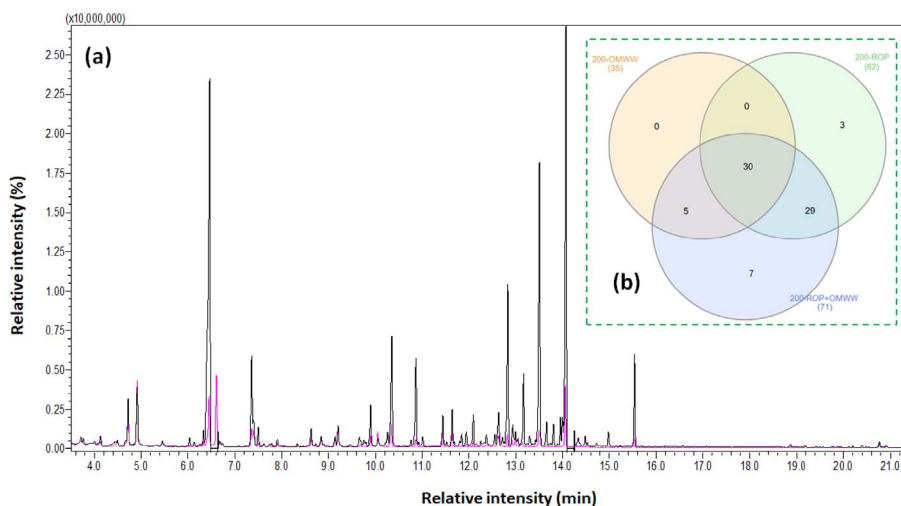
Figure 9. (a) GC–MS profile of 200-ROP (in pink) and 200-ROP + OMWW (in black) and (b) the relative Venn diagram representing the number of common and exclusive organic compounds for 200-ROP, 200-OMWW, and 200-ROP + OMWW [60].

a large variety of chemical species are detected such as phenolic and heteroaromatic compounds in addition to a major quantity of carboxylic acids and monosaccharides. The only types of compounds characterized in the literature after the HTC of ROP are generally furfural and 5-HMF obtained by lignin and cellulose degradation, respectively, and some phenolic compounds such as vanillin, 4-hydroxy-3-methoxyphenylacetone (guaiacylacetone), 2,6-dimethoxyphenol (syringol), syringaldehyde, guaiacol, acetosyringone, phenol, 1-(4-hydroxy-3-methoxyphenyl)-ethanone (acetovanillone), creosol, and 1-(2,4,6-trihydroxyphenyl)-2-pentanone [61,62]. In this paper, a comparison is performed for liquid fractions from HTC experiments at 200 °C. Here, the use of OMWW instead of DW for the HTC of ROP leads to a significantly different GC–MS profile as presented in Figure 9a. Moreover, as we compare these results with the 200-OMWW profile (data published previously [10]), we can note that among the 74 detected compounds, 30 are present in all three modalities and thus emerge from both OMWW and ROP after HTC (Figure 9b). Moreover, 29 compounds are present in 200-ROP and 200-ROP + OMWW samples and are specific to ROP. The five compounds found in 200-OMWW and 200-ROP + OMWW arise from OMWW, while 10 compounds arise from ROP. However, for these last compounds, we distinguish

seven molecules, which are observed only when ROP HTC is conducted in the presence of OMWW. The remaining three are lost or transformed in the presence of OMWW.

The sum of relative areas for the 29 molecules detected only in 200-ROP and 200-ROP + OMWW is presented in Figure 10. Accordingly, higher contents are obtained in the different chemical classes, in particular for cyclic carboxylic acid and heterocyclic compounds. Such results suggest that a better HTC of ROP can be predicted in the presence of OMWW rather than DW. Similar outcomes are obtained at the other temperatures of 180 and 220 °C.

Moreover, seven molecules are detected only when HTC of ROP is performed in the presence of OMWW and, notably, the putative compound salidroside, which is a glucosylated form of tyrosol. It is well known that tyrosol is a major component of olive oil [63] and is abundant in OMWW-derived hydrochars [64]. We detected tyrosol in all T-ROP samples and in very higher proportions in raw OMWW, T-OMWW, and T-ROP + OMWW [10]. On the other hand, glucose is only identified in raw OMWW, suggesting that glucose is degraded via the HTC process. Therefore, the existence of salidroside can be explained in terms of the coupling between glucose and tyrosol when olive stones and raw OMWW are
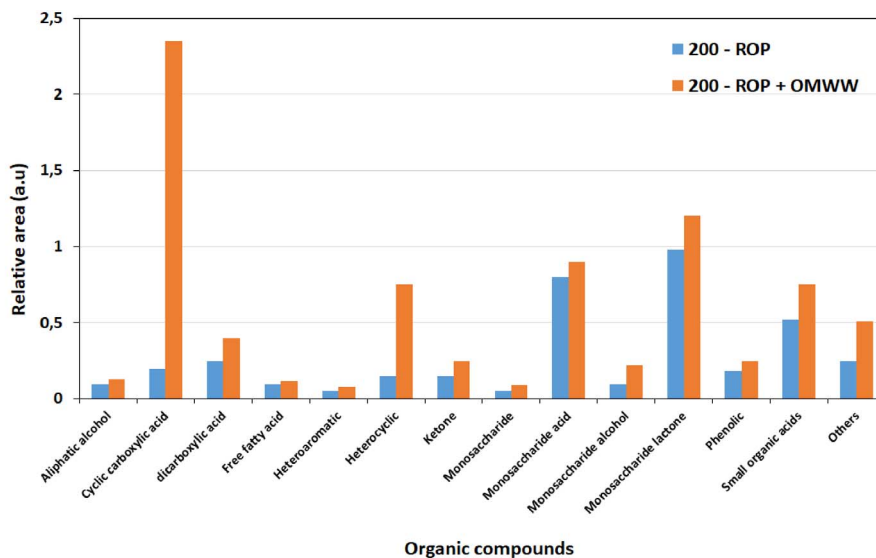
Figure 10. Sum of normalized areas of the different chemical compound classes detected after HTC of ROP in the presence of distilled water and OMWW at 200 °C.

copresent. A similar explanation can be applied for the formation of monoacetin (glycerol monoacetate) since glycerol is much more abundant in OMWW than in ROP.

4. Conclusions

This research has investigated the possible conversion of hazardous OMWW to an environmental-friendly substitute for water in the HTC of ROP into carbon-rich materials. The utilization of OMWW considerably enhanced some mineral contents, especially potassium and magnesium. Moreover, the carbonization of ROP in the presence of OMWW instead of DW at 220 °C enhanced the HHV by approximately 31%. This could be related to the significant increase in C contents and the decrease in O% owing to the acidic nature of the liquid waste. Furthermore, the coapplication of ROP and OMWW enhanced the quality of the final liquid fraction with a significant decrease in the COD value of approximately 53% to 62%. This feature, however, caused significant modifications of some chemical and morphological aspects of the hydrochars. In fact, the use of OMWW instead of DW led to decreases in ash and fixed carbon percentages of 4% and 10%. An increase of 14% in volatile matter contents was noted for 220-ROP

and 220-ROP + OMWW, respectively. Moreover, the use of DW as the carbonization medium ensured the formation of spherical carbon structures with mean diameters varying between 1.09 and 0.62 μm for 180-ROP and 200-ROP, respectively. However, their formation is not favored in the presence of OMWW due to its low pH value. This work demonstrates a circular and environmental-friendly approach to waste management, which may open the door to several possible applications of the solid fractions obtained. Hydrochars produced with DW could be applied as adequate feedstock for the manufacture of high-value-added carbon materials for energy storage applications or as adsorbents in liquid and gaseous media. On the other hand, OMWW-derived hydrochars have properties that make them not only apt for energy generation but also an appropriate source of fixed carbon content for agricultural applications.

Acknowledgments

wish to thank all the personnel operating the technical platforms of the IS2M for their scientific contributions and for their help in running the well-conducted experiments and analyses.

Supplementary data

Supporting information for this article is available on the journal's website under https://doi.org/10.5802/crchim.61 or from the author.

References

[1] A. Méndez, G. Gascó, B. Ruiz, E. Fuente, *Bioresour. Technol.*, 2019, **275**, 386-393.

[2] A. A. Zorpas, V. J. Inglezakis, *Appl. Environ. Soil Sci.*, 2011, **2011**, 1-14.

[3] J. Mata-Alvarez, *Biomethanization of the Organic Fraction of Municipal Solid Wastes, Vol. 4*, Water Intell. Online, 2015.

[4] O. P. Karthikeyan, C. Visvanathan, *Rev. Environ. Sci. Bio/Technol.*, 2013, **12**, 257-284.

[5] K.-H. Yeoh, S. A. Shafie, K. A. Al-attab, Z. A. Zainal, *Bioresour. Technol.*, 2018, **265**, 365-371.

[6] C. Karakaş, D. Özçimen, B. İnan, *J. Anal. Appl. Pyrolysis*, 2017, **125**, 17-23.

[7] S. O. Masebinu, E. T. Akinlabi, E. Muzenda, A. O. Aboyade, *Renew. Sustain. Energy Rev.*, 2019, **103**, 291-307.

[8] D. Bhatt, A. Shrestha, R. Dahal, B. Acharya, P. Basu, R. MacEwen, *Energies*, 2018, **11**, article no. 2286.

[9] A. A. Azzaz, B. Khiari, S. Jellali, C. M. Ghimbeu, M. Jeguirim, *Renew. Sustain. Energy Rev.*, 2020, **127**, article no. 109882.

[10] A. A. Azzaz, M. Jeguirim, V. Kinigopoulou, C. Doulgeris, M.-L. Goddard, S. Jellali, C. Matei Ghimbeu, *Sci. Total Environ.*, 2020, **733**, article no. 139314.

[11] F. Gao, G. Shao, J. Qu, S. Lv, Y. Li, M. Wu, *Electrochim. Acta*, 2015, **155**, 201-208.

[12] S. Schaefer, V. Fierro, M. T. Izquierdo, A. Celzard, *Int. J. Hydrogen Energy*, 2016, **41**, 12146-12156.

[13] K. Reibe, K.-P. Götz, C.-L. Roß, T. F. Döring, F. Ellmer, L. Ruess, *Soil Biol. Biochem.*, 2015, **83**, 84-87.

[14] F. Valenti, C. Arcidiacono, G. Chinnici, G. Cascone, S. M. C. Porto, *Biofuels, Bioprod. Biorefining*, 2017, **11**, 784-797.

[15] M. Jeguirim, P. Dutournié, A. A. Zorpas, L. Limousy, *Energies*, 2017, **10**, article no. 1423.

[16] M. K. Doula, A. A. Zorpas, V. J. Inglezakis, J. P. Navvaro, D. J. Bilalis, *Environ. Eng. Manag. J.*, 2019, **18**, 1297-1309.

[17] M. Jeguirim, M. L. Goddard, A. Tamosiunas, E. Berrich-Betouche, A. A. Azzaz, M. Praspaliauskas, S. Jellali, *Renew. Energy*, 2020, **149**, 716-724.

[18] P. Dutournié, M. Jeguirim, B. Khiari, M.-L. Goddard, S. Jellali, *Water*, 2019, **11**, article no. 768.

[19] A. Chouchene, M. Jeguirim, A. Favre-Reguillon, G. Trouvé, G. Le Buzit, B. Khiari, F. Zagrouba, *Energy*, 2012, **39**, 74-81.

[20] M. Jeguirim, A. Chouchène, A. F. Réguillon, G. Trouvé, G. Le Buzit, *Resour. Conserv. Recycl.*, 2012, **59**, 4-8.

[21] A. Chouchene, M. Jeguirim, G. Trouvé, A. Favre-Reguillon, G. Le Buzit, *Bioresour. Technol.*, 2010, **101**, 6962-6971.

[22] A. Missaoui, S. Bostyn, V. Belandria, B. Cagnon, B. Sarh, I. Gökalp, *J. Anal. Appl. Pyrolysis*, 2017, **128**, 281-290.

[23] G. Ralf, J. J. Leahy, M. T. Timko, A. Trubetskaya, *Renew. Energy*, 2020, **155**, 347-357.

[24] B. González, J. J. Manyà, *Chem. Eng. Process. - Process Intensif.*, 2020, **149**, article no. 107830.

[25] A. Chouchene, M. Jeguirim, B. Khiari, G. Trouvé, F. Zagrouba, *J. Anal. Appl. Pyrolysis*, 2010, **87**, 168-174.

[26] R Development Core Team, "R: a language and environment for statistical computing", 2020.

[27] T-412, *Moisture in pulp, paper and paperboard, Stand. Off. Method*, Tappi, 2012.

[28] W. Thompson, P. Leege, *Test Methods for the Examination of Composting and Compost*, Composting Council Research and Education Foundation, Raleigh, USA, 1998.

[29] S. Graulis, D. Chateigner, R. T. Downs, A. F. T. Yokochi, M. Quirós, L. Lutterotti, E. Manakova, J. Butkus, P. Moeck, A. Le Bail, *J. Appl. Crystallogr.*, 2009, **42**, 726-729.

[30] A. A. Azzaz, S. Jellali, H. Akrout, A. A. Assadi, L. Bousselmi, *Environ. Sci. Pollut. Res.*, 2016, 1-16.

[31] W. A. Moore, R. C. Kroner, C. C. Ruchhoft, *Anal. Chem.*, 1949, **21**, 953-957.

[32] T. Wang, Y. Zhai, Y. Zhu, C. Li, G. Zeng, *Renew. Sustain. Energy Rev.*, 2018, **90**, 223-247.

[33] L. Li, M. Hale, P. Olsen, N. D. Berge, *Waste Manag.*, 2014, **34**, 2185-2195.

[34] S. Başakçılardan Kabakcı, S. S. Baran, *Waste Manag.*, 2019, **100**, 259-268.

[35] X. Chen, Q. Lin, R. He, X. Zhao, G. Li, *Bioresour. Technol.*, 2017, **241**, 236-243.

[36] A. M. Smith, S. Singh, A. B. Ross, *Fuel*, 2016, **169**, 135-145.

[37] N. Huang, P. Zhao, S. Ghosh, A. Fedyukhin, *Appl. Energy*, 2019, **240**, 882-892.

[38] M. T. Elaieb, A. Khouaja, M. L. Khouja, J. Valette, G. Volle, K. Candelier, *Waste Biomass Valorization*, 2018, **9**, 1199-1211.

[39] D. Özçimen, A. Ersoy-Meriçboyu, *Renew. Energy*, 2010, **35**, 1319-1324.

[40] C. Zhao, E. Jiang, A. Chen, *J. Energy Inst.*, 2017, **90**, 902-913.

[41] A. Funke, F. Ziegler, *Biofuels, Bioprod. Biorefining*, 2010, **4**, 160-177.

[42] T. Mathimani, N. Mallick, *J. Clean. Prod.*, 2019, **217**, 69-84.

[43] P. J. Arauzo, L. Du, M. P. Olszewski, M. F. Meza Zavala, M. J. Alhnidi, A. Kruse, *Bioresour. Technol.*, 2019, **293**, article no. 122117.

[44] I. Miranda, R. Simões, B. Medeiros, K. M. Nampoothiri, R. K. Sukumaran, D. Rajan, H. Pereira, S. Ferreira-Dias, *Bioresour. Technol.*, 2019, **292**, article no. 121936.

[45] S. Lammi, A. Barakat, C. Mayer-Laigle, D. Djenane, N. Gontard, H. Angellier-Coussy, *Powder Technol.*, 2018, **326**, 44-53.

[46] P. Biller, A. B. Ross, "Production of biofuels via hydrothermal conversion", in *Handbook of Biofuels Production*, Processes and Technologies, Woodhead Publishing, Oxford, UK, 2nd ed., 2016, 509-547.

[47] S. Kang, X. Li, J. Fan, J. Chang, *Ind. Eng. Chem. Res.*, 2012, **51**, 9023-9031.

[48] M. L. Hobbs, P. T. Radulovic, L. D. Smoot, *Fuel*, 1992, **71**, 1177-1194.

[49] M. Sevilla, A. B. Fuertes, *Carbon N. Y.*, 2009, **47**, 2281-2289.

[50] Q. Wang, F. Cao, Q. Chen, C. Chen, *Mater. Lett.*, 2005, **59**, 3738-3741.

[51] J. Ryu, Y. W. Suh, D. J. Suh, D. J. Ahn, *Carbon N. Y.*, 2010, **48**, 1990-1998.

[52] M. Li, W. Li, S. Liu, *Carbohydr. Res.*, 2011, **346**, 999-1004.

[53] J. Liang, Y. Liu, J. Zhang, *Proc. Environ. Sci.*, 2011, **11**, 1322-1327.

[54] V. K. Lamer, R. H. Dinegar, *J. Am. Chem. Soc.*, 1950, **72**, 4847-4854.

[55] J. Xiong, Z. Pan, X. Xiao, H. Huang, F. Lai, J. Wang, S. Chen, *J. Anal. Appl. Pyrolysis*, 2019, **144**, article no. 104692.

[56] P. A. Nakata, *Plant Sci.*, 2003, **164**, 901-909.

[57] V. R. Franceschi, P. A. Nakata, *Annu. Rev. Plant Biol.*, 2005, **56**, 41-71.

[58] L. Zhang, Q. Wang, B. Wang, G. Yang, L. A. Lucia, J. Chen, *Energy Fuels*, 2015, **29**, 872-876.

[59] S. Guo, X. Dong, T. Wu, F. Shi, C. Zhu, *J. Anal. Appl. Pyrolysis*, 2015, **116**, 1-9.

[60] H. Heberle, V. G. Meirelles, F. R. da Silva, G. P. Telles, R. Minghim, *BMC Bioinformatics*, 2015, **6**, article no. 169.

[61] A. M. Borrero-López, E. Masson, A. Celzard, V. Fierro, *Ind. Crops Prod.*, 2020, **151**, article no. 112452.

[62] A. M. Borrero-López, V. Fierro, A. Jeder, A. Ouederni, E. Masson, A. Celzard, *Environ. Sci. Pollut. Res.*, 2017, **24**, 9859-9869.

[63] G. Purcaro, R. Codony, L. Pizzale, C. Mariani, L. Conte, *Eur. J. Lipid Sci. Technol.*, 2014, **116**, 805-811.

[64] J. Poerschmann, I. Baskyr, B. Weiner, R. Koehler, H. Wedwitschka, F. D. Kopinke, *Bioresour. Technol.*, 2013, **133**, 581-588.

[65] International Organization for Standardization, "Soil Quality: Determination of Total Nitrogen: Modified Kjeldahl Method", 1995, ISO 11261:1995.

[66] A. R. K. Gollakota, N. Kishore, S. Gu, *Renew. Sustain. Energy Rev.*, 2018, **81**, 1378-1392.

[67] E. Atallah, W. Kwapinski, M. N. Ahmad, J. J. Leahy, A. H. Al-Muhtaseb, J. Zeaiter, *J. Environ. Chem. Eng.*, 2019, **7**, article no. 102833.

[68] V. Benavente, A. Fullana, N. D. Berge, *J. Clean. Prod.*, 2017, **142**, 2637-2648.

[69] E. Atallah, W. Kwapinski, M. N. Ahmad, J. J. Leahy, J. Zeaiter, *J. Water Process Eng.*, 2019, **31**, article no. 100813.

[70] J. Poerschmann, B. Weiner, I. Baskyr, *Chemosphere*, 2013, **92**, 1472-1482.